Red light activatable chemo-optogenetic dimerization regulates cell apoptosis

Yue Zhou[1], Chengjian Zhou[1,2], Ziqi Zhou[1,2], Yan Zhang[1,2], Xi Chen[1,2,*]

[1] Laboratory of Chemical Biology and Frontier Biotechnologies, The HIT Center for Life Sciences, Harbin Institute of Technology, Harbin City, P.R. China 150001

[2] School of Life Science and Technology, Harbin Institute of Technology, Harbin, P.R. China 150001

*Email: chenxihit@hiti.edu.cn

Abstract

We report a non-phototoxic and non-photobleaching chemo-optogenetic dimerizer that effectively regulates protein-protein proximity inside living cells using far-red light. This system introduced the first deep-red/NIR light photoactivatable chemical inducer of proximity (pCIP) or dimerization (pCID), called dmBODIPY-ABA, or dmBODIPY caged abscisic acid (ABA). dmBODIPY-ABA dimerizer shows an anti-Stokes feature that further shifts the absorption to NIR direction and it displays a strong hyperchromic shift compared to the dmBODIPY photocage. By utilizing this non-invasive and biocompatible system, we successfully controlled apoptosis by targeting the key apoptotic factor, Bax, to the outer membrane of mitochondria, thus opening a window for precise control of programmed cancer cell death using deep-red light.

Keywords: abscisic acid, apoptosis, chemically induced dimerization, chemo-optogenetic, BODIPY, deep-red light

Introduction

Light control of cellular processes is highly advantageous due to its high spatial resolution, precise temporal control, and non-invasive nature[1, 2]. Chemical biologists have adopted chemo-optogenetics, known as a 'chemistry' version of optogenetics, to regulate various cellular functions[3-8]. Unlike optogenetics, which utilizes genetically encoded photoreceptors[9] or light-sensitive ion channels[10], chemo-optogenetic tools, such as photoactivatable chemical inducers of dimerization (pCIDs), employ genetically engineered protein tags that specifically accept light-sensitive small molecules[2, 11]. Therefore, it is a versatile and a general approach for optically controlling cellular functions with minimal off-target effects on other proteins or cellular pathways. In comparison to optogenetic methods, chemo-optogenetic tools facilitate stronger interactions, exhibit minimal basal activities, are compatible with multi-color imaging, have a high dynamic range, and can be implemented in a standard confocal microscope without the need for additional sophisticated illumination devices[2, 12, 13].

Currently available chemo-optogenetic tools primarily utilize ultraviolet or violet 405 nm irradiation, which can be highly phototoxic and cause inevitable bleaching to fluorescent proteins. However, the use of shorter wavelengths of light, even up to the green-color

spectrum, has limited potential in translational applications in tissue or in vivo due to poor tissue penetration. Therefore, it would be highly advantageous to use longer wavelengths of light such as deep/far-red (> 630 nm) and near infrared (NIR) light (>700 nm) that fall within biological windows[14]. Deep-red light can readily penetrate tissues, is not phototoxic, and minimally bleaches widely used fluorescent proteins. Thus, in this study, we aimed to introduce a deep-red light activatable chemo-optogenetic system for controlling cellular functions.

Apoptosis is a major form of programmed cell death that plays a crucial role in maintaining physiological homeostasis in almost every organ system[15]. It is mediated by a series of effectors, including caspases and other regulators, which selectively eliminate unwanted cells in an organism (**Fig. 1a**). Research has shown that certain cancer cells, such as HGPIN (proliferation of glandular epithelium) and prostate carcinoma, exhibit significantly higher levels of apoptosis compared to normal cells. Therefore, it has been suggested that selectively inducing apoptosis could be a promising approach to treating cancer[16]. Considering the exceptional spatial precision offered by optical control, the utilization of deep-red light chemo-optogenetic tools to regulate apoptosis may hold great potential for selectively inducing cancer cell death[17].

Results and discussion

As the first step, we aimed to design a deep-red light responsive chemo-optogenetic dimerizer. So far, a plethora of chemical inducers of dimerization (CIDs) or chemical

inducers of proximity (CIPs) molecules have been reported that bring protein tags in close proximity to regulate cellular functions[18] They are either naturally occurring small molecules being orthogonal to mammalian cells or synthetically prepared to bear additional new features. After examining known CID and CIP molecules[18, 19], we realized that (+)-abscisic acid (ABA) appears to be the idealist candidate. ABA is a plant hormone that binds with the PYL protein to form a complex and subsequently recognizes ABI domain[9]. As a dimerizer, ABA is small, readily cell permeable, orthogonal to mammalian cell systems, and induces the heterodimerization between PYL and ABI with a high dynamic range. More importantly, ABA features an *α,β,γ,δ*-unsaturated carboxylate and an *α,β*-unsaturated ketone that are essential for inducing proximity (**Fig. 1a**); and the planar feature of the two *π*-systems have already been validated by crystallographic studies[20]. We envisioned that, after introducing a *π*-rich red-absorbing photocage, (+)-ABA may further shift the photo-uncaging wavelength to NIR direction via intramolecular *π*-*π* stacking interactions[21, 22] and creates a true deep-red or even NIR responsive chemo-optogenetic dimerizer.

Only until recently, red light responsive photocages with enhanced quantum yields were introduced[23]. Among them, we identified two red-absorbing BODIPYs as possible candidates to design our chemo-optogenetic system. The two BODIPY cages, namely *B*,*B*-dimethyl-BODIPY (i.e., dmBODIPY, when R = Me) or *B*,*B*-difluoro-BODIPY (i.e. dfBODIPY, when R = F) were prepared in several steps from commercially available starting materials (**Scheme S1**). Afterwards, classical esterification coupling reactions between (+)-ABA and BODIPY cages create two photo-activatable dimerizers—dmBODIPY-ABA and dfBODIPY-

ABA (**Fig. 1b**). Unlike the traditional difluoro-substituted BODIPYs, the dmBODIPY photocage is characterized by dimethyl substitution at the boron atom, a feature that is considered to significantly enhance photouncaging quantum yield by blocking unproductive conical intersections[24]. On the other hand, the dfBODIPY cage is assumed to display absorptions at more red-shifted region than dmBODIPY. After BODIPY-ABA photoactivatable proximity inducers enter a live cell, it may induce the proximity between protein A fused with ABI and protein B fused with PYL-tag upon deep-red light illumination (**Fig. 1c**).

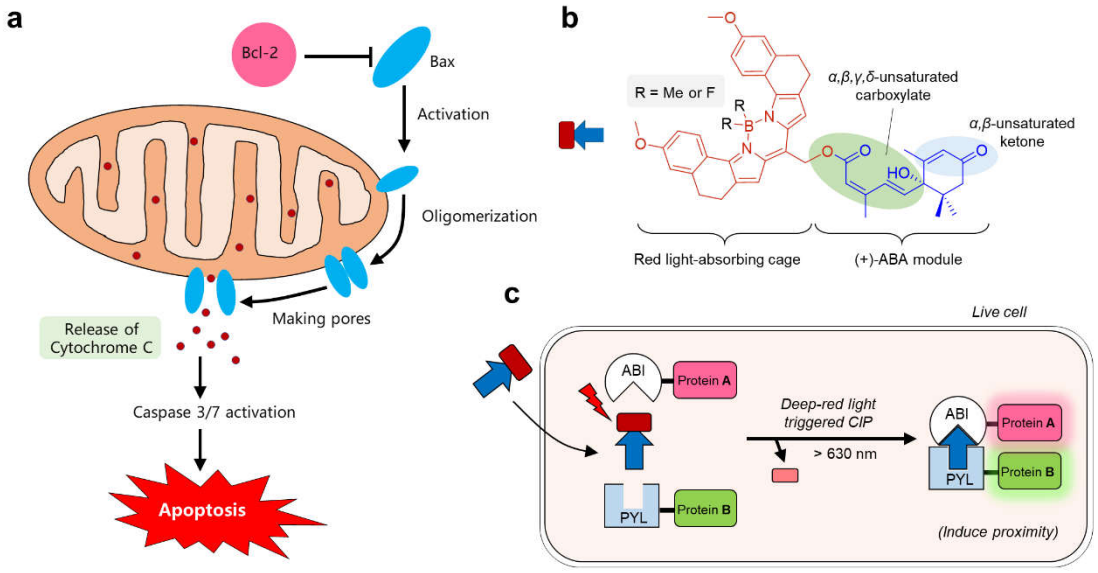

Figure 1. Schematic view of apoptosis and design of a photoactivatable chemo-optogenetic system for control of proximity inside living cells by deep-red light. a) Schematic view of the apoptotic pathway where the apoptotic factor Bax protein plays a key role. b) The structural elements of dmBODIPY-ABA (when R = Me) and dfBODIPY-ABA (when R = F); the characteristic *α,β,γ,δ*-unsaturated carboxylate and *α,β*-unsaturated ketone elements in (+)-ABA module were highlighted. c) Schematic view of how proximity between protein A and B was induced inside living cells by deep-red light using BODIPY-

ABAs.

We next studied the photophysical properties of BODIPY-ABAs and their respective BODIPY photocages (**Fig. 2**). UV-vis absorption spectra show that dmBODIPY-ABA has an absorption maximum at 670 nm in the deep-red region with a high molar extinction coefficient of ε=9.32×10^4 M^{-1}·cm^{-1} in serum-containing imaging medium which mimics physiological environment (**Fig. 2a**). Interestingly, dmBODIPY-ABA shows an emission spectrum (λ_{em} 651 nm) at a shorter wavelength than its absorption spectrum (λ_{max} 670 nm) with an anti-Stokes shift of ~20 nm. Moreover, dmBODIPY-ABA shows a strong hyperchromic shift with an extinction coefficient (ε=9.32×10^4 M^{-1}·cm^{-1}) that is around 3 times higher than dmBODIPY cage (ε=3.15×10^4 M^{-1}·cm^{-1}). These results demonstrate that the attachment ABA dimerizer to dmBODIPY leads to a profound impact on the photophysical properties of dmBODIPY cage. And this effect is beneficial for deep-red light uncaging in terms of both shifting the absorption to NIR direction and increasing the absorbance to over one orders of magnitutue.

As for dfBODIPY-ABA, it displays an absorption spectrum in NIR region (λ_{max} 701 nm) and all the way to the infrared region (>760 nm) with an extinction coefficient of ε=4.01×10^4 M^{-1}·cm^{-1}. Similar to dmBODIPY-ABA, dfBODIPY-ABA is also an anti-Stokes molecule which reveals an anti-Stokes shift of 20 nm, almost identical to dmBODIPY-ABA. Also, dfBODIPY-ABA displays an hyperchromic shift compared to its cage—dfBODIPY. Because ABA is characterized by its unique planar π-bond-rich elements, we guessed that these effects may be originated from the intramolecular π-π interactions between BODIPY cages

and ABA module, which further delocalized the *π*-clouds of BODOPY photocages. *π*-*π* interactions are more prone to form between electron-deficient and electron-rich modules[21]. Indeed, simulation/calculation of the electrostatic potential maps via molecular modeling reveals that the *π*-systems in ABA are highly electron-deficient while the *π*-systems in BODIPY cages are generally electron-rich (**Fig. S1**). Additionally, the acetic acid (free of delocalized *π*-systems) ester form of BODIPY-cages, i.e. dmBODIPY-OAc and dfBODIPY-OAc, display classical Stokes shifts[24]. These evidences further support that the ABA module indeed cause a beneficial impact on its cage for deep-red light photouncaging, in interms of both red-shifting the absorption and significantly enhancing absoprtion. Hence, we envisioned that the BODIPY-caged ABAs may be appropriate candidates as deep-red/NIR responsive dimerizers to regulate cellular functions.

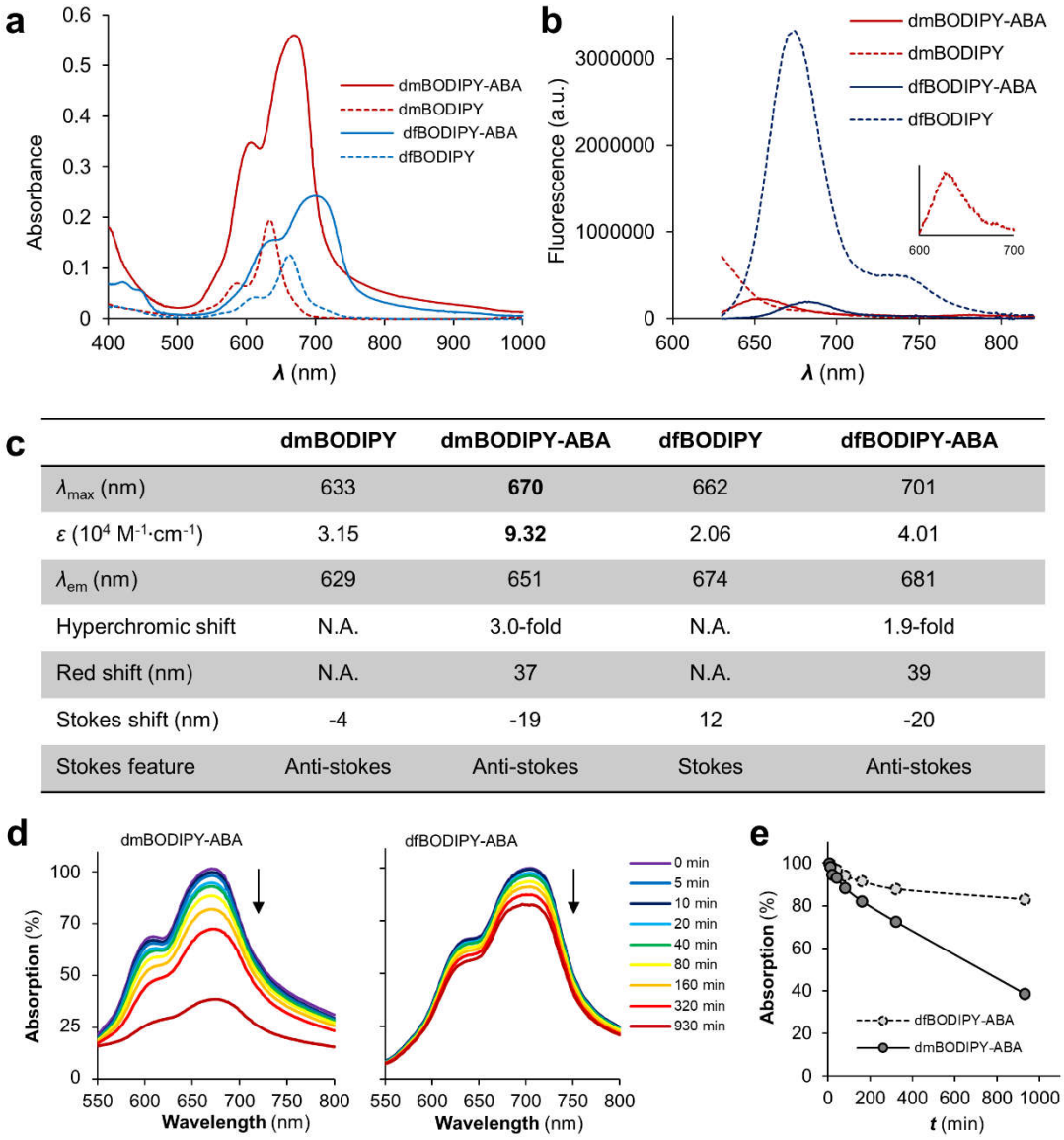

	dmBODIPY	dmBODIPY-ABA	dfBODIPY	dfBODIPY-ABA
λ_{max} (nm)	633	**670**	662	701
ε (10^4 $M^{-1}\cdot cm^{-1}$)	3.15	**9.32**	2.06	4.01
λ_{em} (nm)	629	651	674	681
Hyperchromic shift	N.A.	3.0-fold	N.A.	1.9-fold
Red shift (nm)	N.A.	37	N.A.	39
Stokes shift (nm)	-4	-19	12	-20
Stokes feature	Anti-stokes	Anti-stokes	Stokes	Anti-stokes

Figure 2. Absorption/ fluorescence spectra and photouncaging efficiency analysis. a) UV-Vis absorption spectra. b) Fluorescence emission spectra of the molecules (ex. at 605 nm); the embedded full fluorescence spectrum of dmBODIPY was obtained under excitation at 575 nm (dark-red dashed-line). c) A table that summarizes the photophysical properties of the key molecules in this study. d) Comparison of the photouncaging efficiencies between dmBODIPY-ABA (left) and dfBODIPY-ABA (right) at 20 μM concentration under a deep-red light lamp (660 nm, 8 W); normalized absorption spectra change along with increasing illumination time shows that dmBODIPY-ABA exhibits a higher photouncaging efficiency. e)

The absorption change of dmBODIPY-ABA (at 670 nm) and dfBODIPY-ABA (at 700 nm) was plotted against the illumination doses and the results show that dmBODIPY-ABA is photouncaged much faster than dfBODIPY-ABA. All these experiments were measured in pH 7.2 serum-containing imaging medium that mimics biological cellular environment.

After characterization of the deep-red absorbing dmBODIPY-ABA and NIR absorbing dfBODIPY-ABA, we evaluated if they are able to induce intracellular dimerization and regulate cellular functions by deep-red/NIR light. Mechanistically, dmBODIPY-ABA and dfBODIPY-ABA will release the CIP molecule, (+)-ABA, which subsequently induces the dimerization between ABI and PYL fused proteins[25] upon photouncaging of the BODIPY cages. We first tested if dmBODIPY-ABA and dfBODIPY-ABA induce targeting of protein to the plasma membrane (PM) (**Fig. S2**), a process that has been considered as a general standard to check chemically induced proximity. Live HeLa cells were co-expressed with mCherry-ABI (red, cytosolic) and EGFP-PYL-CAAX (green, PM location). If BODIPY-ABAs are cell permeable and are responsive upon deep-red/NIR light illumination, ABA will be liberated inside living cells and subsequently targets mCherry-ABI to PM location (**Fig. S2a**).

First, live HeLa cells were treated with 10 μM BODIPY-ABAs for 1.5 h, then washed once by PBS. Since both dmBODIPY-ABA and dfBODIPY-ABA exhibit considerable absorptions at 633 nm, we take advantage of the 633 nm He/Ne laser that is equipped in most standard confocal laser scanning microscopes (CLSM) as the illumination source. Increasing doses of 633 nm light illumination were applied to a cell and it could be observed that dmBODIPY-

ABA enabled dose-dependent targeting of mCherry-ABI to PM as revealed by the cell periphery and adhesion spots regions (**Fig. S2b**). For dfBODIPY-ABA, however, no recruitment of mCherry-ABI to PM could be observed even under higher doses of 633 nm laser illumination (**Fig. S2c**). The difference in regulation of protein proximity by deep-red light was further validated by statistical colocalization analysis (**Fig. S2d-e**). Hence, dmBODIPY-ABA is an efficient deep-red light responsive chemo-optogenetic proximity inducer but not dfBODIPY-ABA under the conditions evaluated in our experiment. To further understand this difference, we compared the photouncaging efficiency between dmBODIPY-ABA and dfBODIPY-ABA in imaging medium by determination of their absorption spectrum decrease under deep-red light illumination (**Fig. 2d**). It can be observed that the absorption peaks of dfBODIPY-ABA drop significantly slower than dmBODIPY-ABA (**Fig. 2d-e**), suggesting a compromised photouncaging efficiency of dfBODIPY-ABA compared to dmBODIPY-ABA. Hence, dmBODIPY-ABA is a cell permeable molecule and its chemo-optogenetic system is an ideal photochemical tool to enable temporal control of cellular positionings by deep-red light.

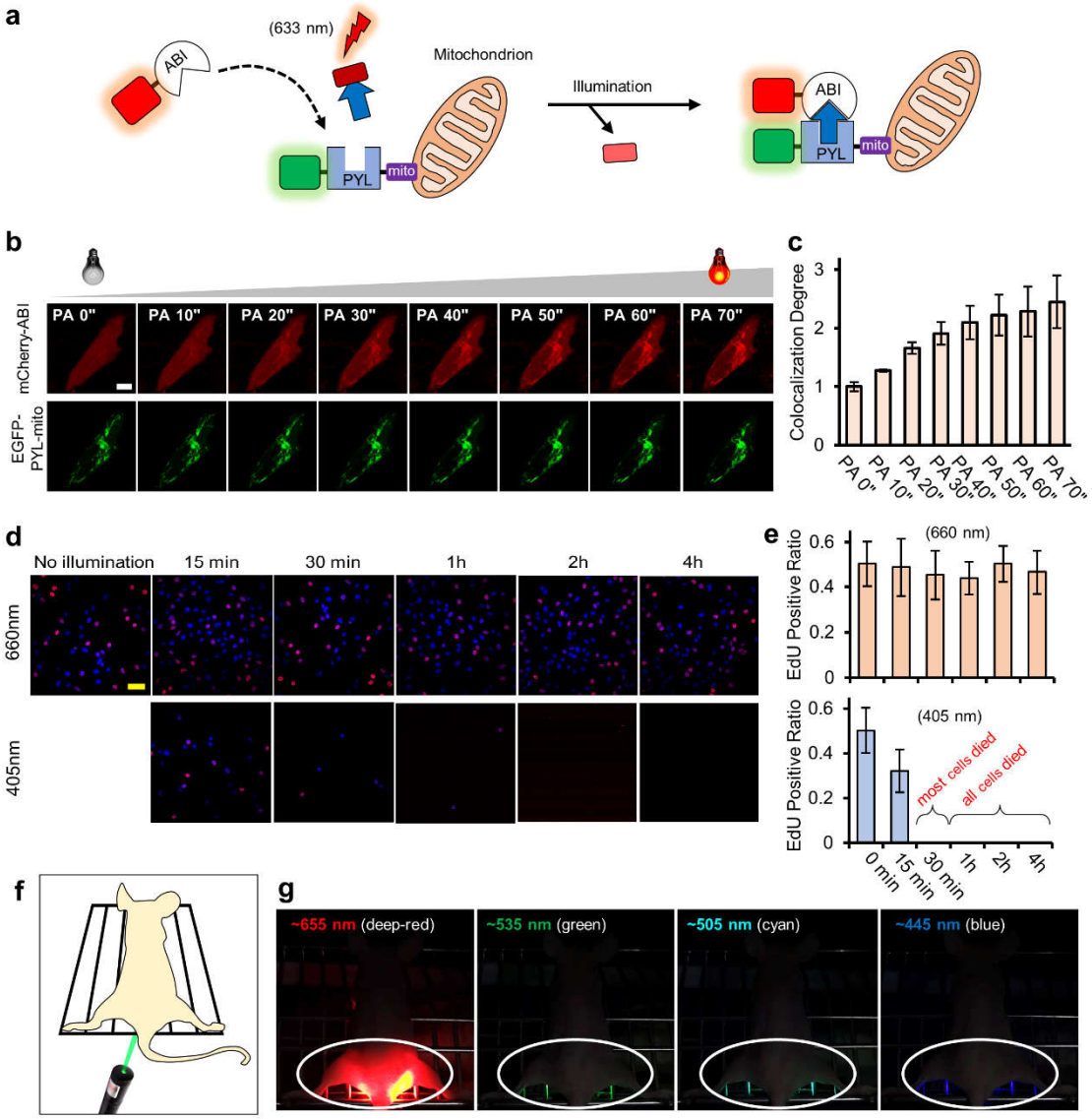

Figure 3. Chemo-optogenetic control of the positioning of a protein onto the surface of mitochondria using dmBODIPY-ABA by deep-red light. a) Schematic view of the experimental design. b) Live HeLa cells coexpressing mCherry-ABI (red, cytosolic) and EGFP-PYL-mito (green, mitochondria) were treated with dmBODIPY-ABA (10 μM, 1.5 h). The HeLa cell was irradiated with increasing doses of 633 nm light, which led to step-wise increased recruitment of mCherry-ABI onto mitochondria. Mito-sequence: ESGDASGSGSGSRAQASNSKLIAKSAEDEKAKEEPGNHRIVILAMLAIGVFSLGALIKIIQL RKNN. c) Normalized statistical colocalization degree (Pearson's coefficient) between the

two channels (n=3; error bars: SEM). d) EdU cell proliferation assay of two groups of live HeLa cells under different doses of deep-red light or 405 nm violet light irradiation. Hoechst was used to stain the cells and the number of blue nuclei reveals the entire cell numbers while those EdU-positive cells (i.e. S-phase cells) were labeled in red. e) Statistical analysis of the EdU positive ratios of deep-red light and 405 nm light illuminated cells (n=10 fields; error bars: SD); note that 405 nm light not only significantly inhibited cell proliferation, but also killed most cells in 30 min. f) Cartoon representation of the experimental setup. f) Photographs of the mice illuminated with different colors of laser light, which revealed that deep-red light showed deep tissue penetration while other colors of light display only poor tissue penetration. Scale bars: white, 10 μm; yellow, 50 μm.

With the success above, we were motivated to see if dmBODIPY-ABA is able to target proteins to the outer membrane of mitochondria, which will pave the way to control programmed cell death mediated by mitochondria (**Fig. 3a**). In this regard, HeLa cells were coexpressed with mCherry-ABI (red, cytosolic) and EGFP-PYL-mito (green, mitochondria). Mito is a mitochondrial targeting sequence that localizes at the outer membrane of mitochondria. After treatment of HeLa cells with dmBODIPY-ABA (10 μM, 1.5 h) and wash (1×PBS), HeLa cells were illuminated with increasing doses of 633 nm laser light. As can be seen from the confocal microscopic images, mCherry-ABI was gradually targeted to mitochondria along with increasing doses of 633 nm laser irradiation (**Fig. 3b**). Statistical Pearson's correlation coefficient (PCC) analysis further showed that the colocalization between mCherry and EGFP channels was increased significantly after applying light

illumination (**Fig. 3c**). Hence, dmBODIPY-ABA-based photo-proximity inducing system is able to target protein factors to the surface of mitochondria by deep-red light.

It is worthy to note that no bleaching of either mCherry channel or EGFP channel was observed, suggesting that this chemo-optogenetic tool is a non-photobleaching system. We then checked that if the deep-red light we used is toxic or not to live cells using EdU cell proliferation assay (**Fig. 3d**). EdU assay is currently acknowledged as one of the best ways to sensitively and robustly determine a cell's proliferation activity. 5-Ethynyl-2'-deoxyuridine (EdU) is a thymidine analog that can be incorporated into newly synthesized DNAs by cells and the ethynyl group allows subsequent click labeling of an azido-fluorophore. Hence, a cell showing a brighter fluorescence at the nucleus indicates a higher proliferation activity. We used either violet light (405 nm), a most widely used photoactivation wavelength, and a deep-red light (~660 nm) of similar watts (~ 8 W) to illuminate live HeLa cells. As can be seen, deep-red light illumination resulted in no detectable phototoxicity to the live cells at all. Also, no cell death was observed nor any proliferation activity was inhibited (**Fig. 3d-e**). In a sharp contrast, 405 nm light kills most cells within 15 min of illumination and live cells were almost completely eradicated after 30 min of illumination (**Fig. 3d-e**). This experiment provides evidences that deep-red light is highly advantageous over violet light in biological applications by preventing cells from photo-toxicity damages. Moreover, we also showed that deep-red light has a much better tissue penetration that other wavelengths of light. Using live mice as the animal model (**Fig. 3f**), we can see that deep-red light penetrates mice tissues deeply whereas green, cyan and blue color light show very poor tissue penetration (**Fig. 3g**). Hence, dmBODIPY-ABA

proximity inducer enables the recruitment of protein factors onto mitochondria surface using non-phototoxic, non-photobleaching and deep-penetrating deep-red light.

Finally, we applied our deep-red chemo-optogenetic system to regulate programmed cell death. As illustrated above, apoptosis requires a key factor called Bax protein (**Fig. 1a**). Under normal conditions, Bax is cytosolic and is inhibited by Bcl2[26]. If Bax is activated, it will be targeted onto mitochondria, undergoes oligomerization and allows Bax making pores on mitochondria to release the cell killer factor—cytochrome C. Cytochrome C subsequently stimulates apoptosis through caspase 3/7 activation[27]. Therefore, we envisioned that direct targeting of Bax onto mitochondria may be a feasible way to regulate this programmed cell death. Hence, we cloned Bax-mCherry-ABI and EGFP-PYL-mito and co-expressed them in live HeLa cells (**Fig. 4a**). Then live HeLa cells were treated with 20 μM dmBODIPY-ABA for 1.5 h, washed and illuminated with increasing doses of 633 nm light. It can be seen from the confocal microscopic images that Bax protein was recruited to mitochondria in a dose-dependent manner (**Fig. 4b**). After 60 s of illumination time, significant morphological changes of mitochondria were observed (**Fig. 4c**), and meanwhile, the entire cell shape was also changed, most noticeably, the shrinkage of the cell (**Fig. 4d**). A close-up view of mitochondria showed that the original linear shaped mitochondria started to shrink, swell and exhibit clear pores (**Fig. 4e**). Statistical colocalization analysis also revealed that Bax protein was recruited to mitochondria during the apoptotic processes (**Fig. 4f**); and statistical analysis of the cell coverage area further ascertains shrinkage of the cell (**Fig. 4g-h**). A time-lapse video provides a more vivid view

of this deep-red light triggered apoptotic process and the observed features matched well with an apoptotic cell (**Supplementary video 1**). In order to exclude the possibility that the 633 nm light or the dmBODIPY-ABA may cause the apoptotic effect, we performed a control experiment using EGFP-mito instead of EGFP-PYL-mito. Under the same experimental conditions, no recruitment of Bax was observed nor any apoptotic phenomenon was identified (**Fig. S3**). Hence dmBODIPY-ABA allows temporal control of apoptotic cancer cell death via illuminating the non-phototoxic deep-red light.

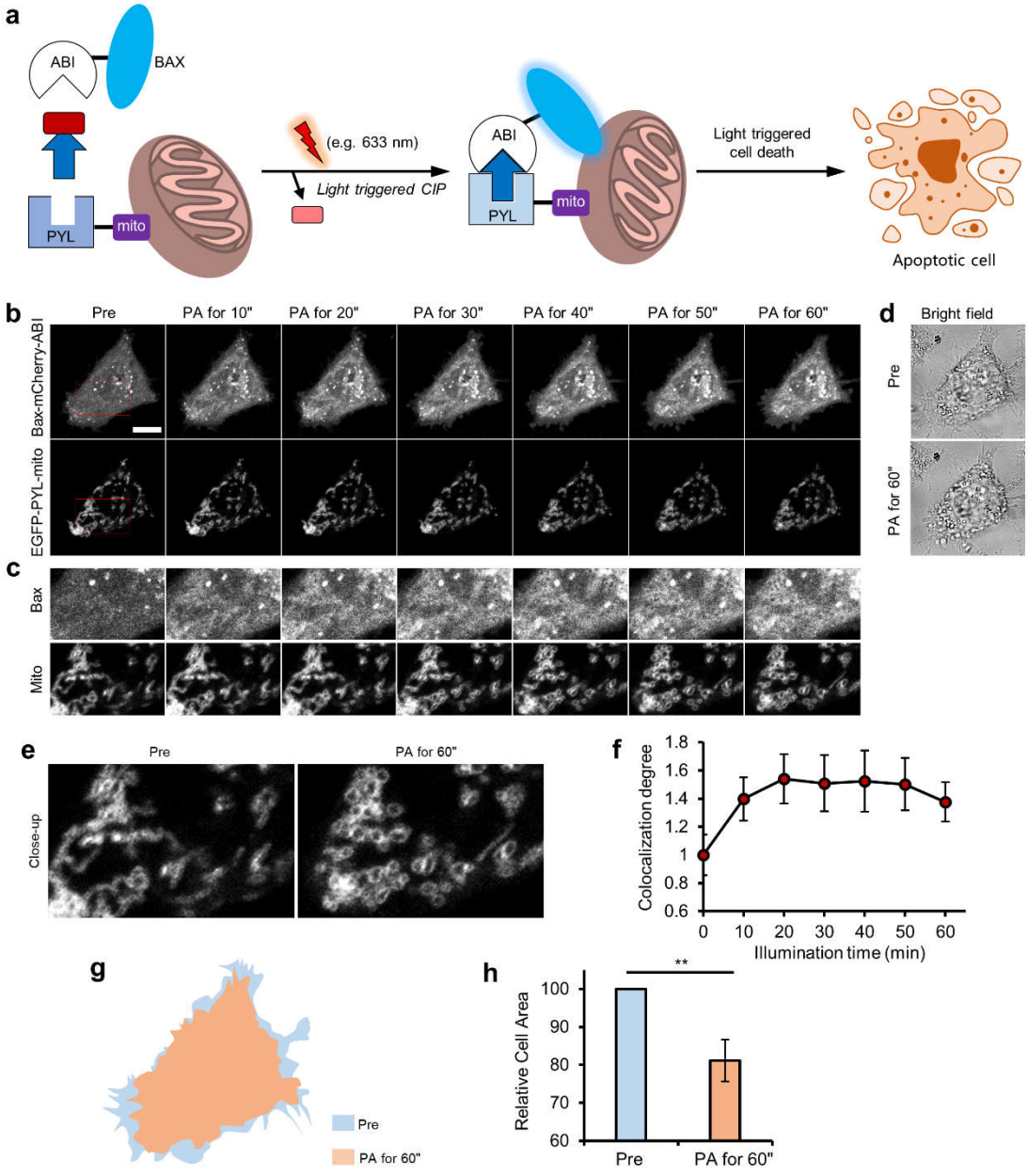

Figure 4. Chemo-optogenetic triggering of apoptosis of cancer cells using 633 nm light. a) Schematic view of how dmBODIPY-ABA based chemo-optogenetic system triggers apoptosis by bringing the apoptotic factor Bax protein to the proximity of mitochondria surfaces. b) Confocal microscopic view of a live HeLa cells coexpression of Bax-mCherry-ABI (red, mainly cytosolic) and EGFP-PYL-mito (green, mitochondria surface) before photoactivation (Pre) and after applying gradient doses of 633 nm irradiation. c) Close-up visualization of Bax recruitment and morphological change of mitochondria. d) Bright-field images of the cell revealed clear shrinkages. e) Morphological change of mitochondria before PA (Pre) and after PA. f) Statistical analysis of the normalized colocalization degree (Pearson's coefficient) between the two channels (n=4; error bars: SEM). g) Cartoon representation of the cell overage surfaces before PA (Pre, light blue) and after PA (light orange), which clearly revealed the shrinkage of the cell after 633 nm light activation. h) Statistical analysis of the normalized cell coverage areas before PA (Pre) and after PA (n=4; error bars: SD). All scale bars: 10 μm.

Conclusions

In all, we have introduced a non-phototoxic and non-photobleaching anti-Stokes chemo-optogenetic system that utilizes deep-red light to induce proximity within living cells. The key component of this system is a photoactivatable chemical inducer of proximity called dmBODIPY-ABA. A comparison between dmBODIPY-ABA and dfBODIPY-ABA suggests that achieving sufficient photouncaging efficiency is crucial for the successful establishment of this deep-red light control system. Unlike the dmBODIPY cage,

dmBODIPY-ABA exhibits an anti-Stokes feature, with its absorption wavelength higher than its emission wavelength. This anti-Stokes feature is particularly advantageous for bio-applications due to its red-shifted absorption spectra[28]. By utilizing the dmBODIPY-ABA-based system, we were able to optically modulate apoptosis in cancer cells using deep-red light. Although in vivo experiments of this system were not conducted in the current study, we have demonstrated the ability to control programmed cell death and highlighted the benefits of deep-red light. Therefore, we anticipate that this research will open new avenues for manipulating programmed cell death to treat cancers using the biologically benign deep-red light.

Author contributions

X.C. conceived the project, supervised the study, designed experiments, and wrote the manuscript; Y.Z. (Yue Zhou) designed and performed the experiments, analyzed the data, and participated in drafting the manuscript; C.Z performed some experiments and participated in writing the manuscript; Z.Z. performed some experiments; Y.Z. (Yan Zhang) performed some spectra analysis and interpretation, and participated in writing the manuscript.

Acknowledgements

We thank the core facilities at The HIT Center for Life Sciences and School of Life Science and Technology in Harbin Institute of Technology. We would also like to thank Simin Xia for providing assistance with the experiments involving the mouse animal model.

This work was supported by the funding from HIT (to X.C.), Overseas Outstanding Young Talents Program of China (to X.C.), National Natural Science Foundation of China (grant No. 32071410 to X.C.), and Natural Science Foundation of Heilongjiang Province of China (grant No. YQ2022B004 to X.C.).

Competing Interests

The authors declare no competing of interests.

Notes and References

1. Ankenbruck, N., et al., *Optochemical Control of Biological Processes in Cells and Animals.* Angew. Chem. Int. Ed., 2018. **57**(11): p. 2768-2798.

2. Klewer, L. and Y.W. Wu, *Light-Induced Dimerization Approaches to Control Cellular Processes.* Chem. Eur. J., 2019. **25**(54): p. 12452-12463.

3. Yoshii, T., et al., *Chemo-optogenetic Protein Translocation System Using a Photoactivatable Self-Localizing Ligand.* ACS Chem. Biol., 2021. **16**(8): p. 1557-1565.

4. Kamps, D., et al., *Optogenetic Tuning Reveals Rho Amplification-Dependent Dynamics of a Cell Contraction Signal Network.* Cell Rep., 2020. **33**(9).

5. Chen, X. and Y.W. Wu, *Tunable and Photoswitchable Chemically Induced Dimerization for Chemo-optogenetic Control of Protein and Organelle Positioning.* Angew. Chem. Int. Ed., 2018. **57**(23): p. 6796-6799.

6. Sun, H., et al., *Fine-Tuning Protein Self-Organization by Orthogonal Chemo-Optogenetic Tools.* Angew. Chem. Int. Ed., 2021. **60**(9): p. 4501-4506.

7. Lam, P.Y., et al., *TRPswitch-A Step-Function Chemo-optogenetic Ligand for the Vertebrate TRPA1 Channel.* J. Am. Chem. Soc., 2020. **142**(41): p. 17457-17468.

8. Chen, X. and S. Petry, *Chemo-optogenetic control of cytoskeleton function.* Abstr. Pap. Am. Chem. Soc., 2019. **258**.

9. Baumschlager, A., *Engineering Light-Control in Biology.* Front. Bioeng. Biotech., 2022. **10**.

10. Deisseroth, K., *Optogenetics: 10 years of microbial opsins in neuroscience.* Nat. Neurosci., 2015. **18**(9): p. 1213-1225.

11. Chen, X., et al., *"Molecular Activity Painting": Switch-like, Light-Controlled Perturbations inside Living Cells.* Angew. Chem. Int. Ed., 2017. **56**(21): p. 5916-5920.

12. Niu, J., et al., *Following Optogenetic Dimerizers and Quantitative Prospects.* Biophys J., 2016. **111**(6): p. 1132-1140.

13. Chen, X., et al., *Multidirectional Activity Control of Cellular Processes by a Versatile Chemo-optogenetic Approach.* Angew. Chem. Int. Ed., 2018. **57**(37): p. 11993-11997.

14. Vorobev, A.Y. and A.E. Moskalensky, *Long-wavelength photoremovable protecting groups: On the way to in vivo application.* Comput. Struct. Biotec., 2020. **18**: p. 27-34.

15. D'Arcy, M.S., *Cell death: a review of the major forms of apoptosis, necrosis and autophagy.* Cell Biol. Int., 2019. **43**(6): p. 582-592.

16. Carneiro, B.A. and W.S. El-Deiry, *Targeting apoptosis in cancer therapy.* Nat. Rev. Clin. Oncol., 2020. **17**(7): p. 395-417.

17. Zheng, B., et al., *Near-Infrared Light Triggered Upconversion Optogenetic Nanosystem for Cancer Therapy.* ACS Nano., 2017. **11**(12): p. 11898-11907.

18. Stanton, B.Z., E.J. Chory, and G.R. Crabtree, *Chemically induced proximity in biology and*

medicine. Science, 2018. **359**(6380).

19. Voss, S., L. Klewer, and Y.W. Wu, *Chemically induced dimerization: reversible and spatiotemporal control of protein function in cells.* Curr. Opin. Chem. Biol., 2015. **28**: p. 194-201.

20. Yin, P., et al., *Structural insights into the mechanism of abscisic acid signaling by PYL proteins.* Nat. Struct. Mol. Biol., 2009. **16**(12): p. 1230-U42.

21. Chen, T., M.X. Li, and J.Q. Liu, *π−π Stacking Interaction: A Nondestructive and Facile Means in Material Engineering for Bioapplications.* Cryst. Growth Des., 2018. **18**(5): p. 2765-2783.

22. Tauer, T.P., M.E. Derrick, and C.D. Sherrill, *Estimates of the ab initio limit for sulfur-pi interactions: The H2S-benzene dimer.* J. Phys. Chem. A, 2005. **109**(1): p. 191-196.

23. Weinstain, R., et al., *Visible-to-NIR-Light Activated Release: From Small Molecules to Nanomaterials.* Chem. Rev., 2020. **120**(24): p. 13135-13272.

24. Shrestha, P., et al., *Efficient Far-Red/Near-IR Absorbing BODIPY Photocages by Blocking Unproductive Conical Intersections.* J. Am. Chem. Soc., 2020. **142**(36): p. 15505-15512.

25. Liang, F.S., W.Q. Ho, and G.R. Crabtree, *Engineering the ABA Plant Stress Pathway for Regulation of Induced Proximity.* Sci. Signal, 2011. **4**(164).

26. Renault, T.T., et al., *Regulation of Bax mitochondrial localization by Bcl-2 and Bcl-x(L): Keep your friends close but your enemies closer.* Int. J. Biochem. Cell B, 2013. **45**(1): p. 64-67.

27. Jeng, P.S., et al., *BH3-dependent and independent activation of BAX and BAK in mitochondrial apoptosis.* Curr. Opin. Physiol., 2018. **3**: p. 71-81.

28. Zhu, X.J., et al., *Anti-Stokes shift luminescent materials for bio-applications.* Chem. Soc. Rev., 2017. **46**(4): p. 1025-1039.